

Density functional theoretical (DFT) study for the prediction of spectroscopic parameters of ClCCCN.

Pradeep Risikrishna Varadwaj*

Saha Institute of Nuclear Physics, Block-AF, Bidhannagar, Kolkata - 700 064, India

DFT(B3LYP, B3PW91) level calculations in conjunction with three different of basis sets have been used to investigate the variations in the bond lengths, dipole moment and rotational constants, IR frequencies, IR intensities and rotational invariants of ClCCCN. The nuclear quadrupole constants of chlorine and nitrogen of ClCCCN have been calculated on the experimental r_s structure as well as on the B3PW91/6-311++g(d,p) optimized geometry and are found to be within the scale length of the experimental uncertainty. The slopes and intercepts obtained from the regression analysis between the B3LYP/6-311++g(d,p) level calculated and experimental B_o values of ClCCCN were used to calculate the reasonable values of rotational constants of all the rare isotopic species of ClCCCN having standard deviation ± 0.048 MHz. All the spectroscopic parameters obtained from DFT calculation shows satisfactory agreement with the available experimental data.

I. INTRODUCTION

Quantum chemical calculation and spectroscopic characterization of organic compounds, free radicals, radical anions etc. have found considerable amount of interest in recent years^{1,2,3,4}. Accurate and efficient calculation of spectroscopic constants for a wide range of molecular systems employs readily available methods and basis sets^{5,6}. The DFT method has been demonstrated to have great accuracy in reproducing the experimental values of quadrupole hyperfine coupling constants⁷, molecular structural properties⁸, rotational constants^{1,4}, IR frequencies, IR intensities and rotational invariants^{9,10,11} etc. to within 8-10%. DFT studies have been carried out for many compounds like BrCCCN¹², FC₈H¹³, ClCN¹⁴ etc. and benzene derivatives like o-benzyne⁴, 3-chlorobenzonitrile¹⁵ etc. to calculate their accurate spectroscopic parameters. Highest number of the polyatomic molecules identified in space are mostly carbon chains^{16,17}, the longest chain identified so far is HC₁₁N¹⁸. Identification and characterization of these species could have been made by their previously reported spectroscopic parameters. Spectroscopic studies of the related series of molecules containing halogens have been extensively studied^{19,20,21,22}. Recently, we have investigated the variations of the spectroscopic parameters of bromo-cyanoacetylene (BrCCCN) at the HF-SCF and DFT levels in conjunction with a variety of basis sets¹². It was found from the the investigation that DFT-B3LYP/6-311++g(d,p) level calculation is satisfactory in the prediction of bond lengths and rotational constants etc. of BrCCCN when compared against their experimental values. However, to my knowledge, a detailed quantum chemical calculations and molecular properties of chloro-cyanoacetylene (ClCCCN) is very limited. Analysis of the microwave spectra of ClCCCN has been reported by T. Bjorvatten²³. Infrared studies of ClCCCN have been reported by S.J. Cyvin et.al²⁴. Later on, P. Klaboe et.

4000 cm⁻¹.

In this study, the results of DFT (B3LYP, B3PW91) level calculations of optimized molecular geometry, rotational constants, quadrupole coupling constants, IR fundamental frequencies, IR intensities and rotational invariants of ClCCCN are compared against their available experimental data and reported. Linear regression analysis between the B3LYP/6-311++g(d,p) level calculated and experimental B_o values have been made for a reasonable prediction of rotational constants of all the other 22 rare isotopomers of ClCCCN. Due to the lack of quantitative data on the IR intensities in the literature, the rotational invariants^{27,28,29} of ClCCCN have been predicted and discussed here may be helpful in future for the experimental IR spectroscopist in interpreting IR intensities of this molecule. Satisfactory agreements between the calculated and available experimental values of spectroscopic parameters have been found at the B3LYP level and compared with the corresponding values calculated at B3PW91, RHF and MP₂ levels of theory. In addition, a test of the optimization followed by a frequency calculation at the MP₂ level in conjunction with a medium size basis set 6-31G or/and 6-311++g(d,p) predicts two negative frequencies (saddle point of order two) corresponding to the -C≡C-Cl doubly degenerate bending mode (ν_7) and thus it was difficult to calculate the harmonic frequencies of these modes under C_v point group symmetry.

II. COMPUTATIONAL METHODS AND CALCULATIONS

Geometry optimization and quantum chemical calculations were carried out at the restricted HF-SCF method, MP₂ method and Density Functional Theoretical (DFT) method under C_v point group symmetry. The hybrid HF/DFT methods used were Becke's three-parameter method³⁰ with Lee-Yang-Parr correlation (B3LYP), Becke's three parameter exchange with Perdew-Wang

Five different basis sets used during the analysis were Dunning's correlation consistent polarized valence double and triple zeta basis sets aug-cc-PVNZ (N = D, T)³⁴ augmented with a d function, Ahlriches TZV(3df,2p)³⁵ and triple split zeta qualities 6-311++g(d,p) and 6-311+g(df,pd) augmented with p, d and f functions. Tight convergence in stead of default convergence criteria was used with ultrafine integration grid for the calculation of normal mode frequencies. All calculations were carried out by the Gaussian03W suite program package³⁶.

The physical quantities \bar{p}_α , β_α and χ_α are invariant with respect to the rotation of space-fixed coordinate axes which are known as generalized atomic polar tensor charge (GAPT)¹¹, atomic anisotropy and Kings atomic effective charge of α th atom respectively and are useful for interpreting infrared intensities. The components of the (3×3) atomic polar tensor matrix $P_X^{(\alpha)}$ are defined as the first derivatives of the components of molecular dipole moment with respect to the atomic Cartesian displacement co-ordinates of each atom α (=Cl, C and N) of ClCCCN given by:

$$P_X^{(\alpha)} = \begin{pmatrix} \frac{\partial p_x}{\partial x_\alpha} & \frac{\partial p_x}{\partial y_\alpha} & \frac{\partial p_x}{\partial z_\alpha} \\ \frac{\partial p_y}{\partial x_\alpha} & \frac{\partial p_y}{\partial y_\alpha} & \frac{\partial p_y}{\partial z_\alpha} \\ \frac{\partial p_z}{\partial x_\alpha} & \frac{\partial p_z}{\partial y_\alpha} & \frac{\partial p_z}{\partial z_\alpha} \end{pmatrix} = \begin{pmatrix} p_{xx} & p_{xy} & p_{xz} \\ p_{yx} & p_{yy} & p_{yz} \\ p_{zx} & p_{zy} & p_{zz} \end{pmatrix} \dots(1)$$

The generalized atomic polar tensor charges (GAPTs) are nothing but mean dipole derivatives^{27,28} given by:

$$\bar{p}_\alpha = \frac{1}{3} \left(\frac{\partial p_x}{\partial x_\alpha} + \frac{\partial p_y}{\partial y_\alpha} + \frac{\partial p_z}{\partial z_\alpha} \right) \quad (2)$$

such that

$$\sum_\alpha \bar{p}_\alpha = 0 \quad (3)$$

for the neutral molecule ClCCCN. The quantity χ_α known as the effective charge of the α th atom, defined by King and co-workers^{28,29} as:

$$\chi_\alpha^2 = \frac{1}{3} [Tr.(P_X^{(\alpha)} P_X'^{(\alpha)})] = \bar{p}_\alpha^2 + \frac{2}{9} \beta_\alpha^2 \quad (4)$$

where

$$\beta_\alpha^2 = \frac{1}{2} [(p_{xx}^{(\alpha)} - p_{yy}^{(\alpha)})^2 + (p_{yy}^{(\alpha)} - p_{zz}^{(\alpha)})^2 + (p_{zz}^{(\alpha)} - p_{xx}^{(\alpha)})^2] + \frac{3}{2} (p_{xy}^{(\alpha)^2} + p_{yz}^{(\alpha)^2} + p_{xz}^{(\alpha)^2} + p_{zx}^{(\alpha)^2} + p_{yx}^{(\alpha)^2} + p_{zy}^{(\alpha)^2}) \quad (5)$$

The molecular polar tensor of ClCCCN is a juxtaposition of the (3×3) atomic polar tensors given by:

$$P_X = \{P_X^{Cl} | P_X^C | P_X^C | P_X^C | P_X^N\} \quad (6)$$

and is calculated from

$$P_X = P_Q L^{-1} U B + P_\rho \beta$$

where L^{-1} , U and B are matrices³⁷ used for molecular vibrational analysis and P_Q contains the dipole moment derivatives with respect to the normal co-ordinates, which are proportional to the experimental infrared intensities³⁸. P_ρ is the rotation plus translation polar tensor whose elements for a neutral molecule proportional to $\mu/I^{\frac{1}{2}}$ and $\rho = BX$, where μ and I are dipole moment and moment of inertia of the molecule respectively. Atomic polar tensor components were directly calculated by Gaussian03 package.

On the other hand, nuclear quadrupole coupling constants (NQCCs) of chlorine and nitrogen of ClCCCN are calculated by using the electric field gradients (EFGs). The elements of the NQCC tensors χ_{ij} are related to those of the EFG tensors q_{ij} by :

$$\chi_{ij} = (eQ/h)q_{ij} \quad (8)$$

where e is the fundamental electronic charge, h is Plank's constant and $i, j = a, b, c$ are the principal axes of the inertia tensor.

III. RESULTS AND DISCUSSION

Optimization of geometry for each molecule at the restricted HF-SCF and DFT levels were performed in the ground state by single point energy calculation. In each case, stationary points were found and linear geometry of ClCCCN was confirmed. Finally, a frequency calculation following each optimization have been performed in order to check for the existence of a true minimum and to confirm an equilibrium structure. A test of geometry optimization followed by a frequency calculation under C_v point group symmetry at the MP₂ level in conjunction with 6-31g or/and 6-311++g(d,p) basis sets succeeded in locating a stationary point but with two imaginary frequencies (IMAG = 2) corresponding to the -C≡C-Cl doubly degenerate bending mode. This confirms that the stationary point located by the MP₂ level of theory is not a true minimum rather a saddle point of order two on the potential energy surface of ClCCCN which may cause a large deformation to the geometry of the molecule. Similar features have also been reported elsewhere³⁹. So the scan of the potential energy surface should be emphasized in order to characterize the the nature of the saddle point on the potential energy surface of ClCCCN and to check any possible existance of conical intersection between the ground and first excited state. However, the DFT and HF-SCF level calculations were not able predict any imaginary frequencies implying that the stationary point is located at the global minimum of the potential energy hyper-surface. The results of our calculation for bond lengths of ClCCCN are summarized in Table 1. The

TABLE I: Comparison of the molecular optimized geometry (in Å), dipole moment, rotational constant and total energy (a.u.) of ClCCCN (calculated by various methods in conjunction with basis sets of increasing size) with the experimental average r_s values²³.

Method	basis	Cl-C	C≡C	C-C	C≡N	Cl..N	μ/D	B/MHz	³⁵ Cl χ_{aa}	¹⁴ N χ_{aa}	Energy
HF	6-311++g(d,p)	1.6359	1.1809	1.3855	1.1355	5.3378	3.82	1394.78	-81.89	-3.81	-627.5026
	aug-cc-pVDZ	1.6421	1.1881	1.3914	1.1372	5.3588	3.85	1381.38	-80.34	-3.61	-627.4784
	aug-cc-pVTZ	1.6325	1.1780	1.3852	1.1277	5.3234	3.86	1399.53	-82.34	-4.30	-627.5349
MP ₂	6-311++g(d,p)	1.6294	1.2238	1.3705	1.1826	5.4063	4.12	1362.79			-628.1965
B3LYP	6-311++g(d,p)	1.6322	1.2064	1.3647	1.1592	5.3625	4.17	1382.60	-72.82	-3.48	-629.2369
	aug-cc-pVDZ	1.6402	1.2159	1.3721	1.1670	5.3952	4.17	1366.05	-77.31	-2.10	-629.2044
	aug-cc-pVTZ	1.6276	1.2039	1.3643	1.1562	5.3520	4.14	1380.00	-76.10	-3.64	-629.2646
B3PW91	6-311++g(d,p)	1.6232	1.2073	1.3632	1.1595	5.3532	4.19	1387.85	-74.93	-3.38	-629.1045
	aug-cc-pVDZ	1.6312	1.2160	1.3700	1.1671	5.3843	4.13	1371.95	-76.05	-2.84	-629.0762
	aug-cc-pVTZ	1.6196	1.2049	1.3630	1.1567	5.3442	4.16	1392.34	-74.16	-3.54	-629.1332
Expt.		1.6245	1.2090	1.3690	1.1602	5.3627	3.38	1382.328(2)			

TABLE II: Comparison of calculated^a and experimental²³ values of quadrupole coupling constants $\chi_{aa}(= \chi_{zz})$ (in MHz) of ³⁵Cl, ³⁷Cl and ¹⁴N of ClCCCN. The values given in the parentheses are directly calculated without using the scaling factors⁷.

Atoms	$\chi_{r_s}^b$	χ_{B3LYP}	χ_{B3PW91}	$\chi_{Expt.}$
³⁵ Cl	-79.57(-80.39)	-80.67(-81.48)	-79.53(-80.35)	-75±4
³⁷ Cl	-62.94(-63.50)	-63.58(64.14)	-62.68(-63.25)	-62±3
¹⁴ N(³⁵ Cl)	-4.29	-4.30	-4.31	...
¹⁴ N(³⁷ Cl)	-4.30

^a See text for discussion.

^b Ref.²³. Actual bond distances based on the r_s co-ordinates are reported to be 1.6233(31) (1.6256(32)), 1.2086(42) (1.2093(43)), 1.3700(23) (1.3680(21)), 1.1607(10) (1.1596(10)) for Cl-C, C≡C, C-C, C≡N of 35 (and 37) species of ClCCCN respectively.

level calculations highly overestimates Cl-C and C-C bond lengths and underestimates C≡C and C≡N bond lengths, whereas these values calculated at the MP2 level overestimates all these bond lengths when compared against their experimental values. However, the results of DFT-B3LYP, B3PW91 method in conjunction with 6-311++g(d,p) basis set are in rather pleasing agreement with the experimental r_s values. Here, We note a slight overestimation of Cl-C bond length and an underestimation of C≡C and C≡N bond lengths, differences between calculated values and the average r_s values in bond lengths for ClCCCN are 0.0077 Å, -0.0026 Å, -0.0043 Å and -0.001 Å for Cl-C, C≡C, C-C and C≡N respectively at the B3LYP level, whereas a slight underestimation of all these bond distances being noticed at the B3PW91 level of theory, differences are -0.0013 Å, -0.0017 Å, -0.0058 Å, -0.0007 Å for Cl-C, C≡C, C-C and C≡N respectively. A comparison of bond lengths calculated at various levels, summarized in Table 1, indicate that convergence has not achieved on improving the size of the basis sets 6-311++g(d,p) to aug-cc-PVTZ. However, a better comparison is made on the over-all (end-over-end) length, $r_{Cl...N}$, of the molecule which is

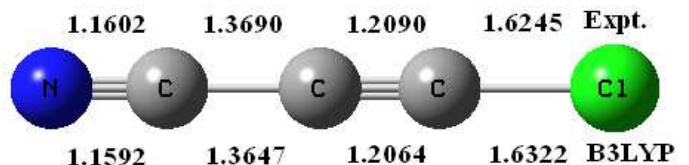


FIG. 1: Comparison between the calculated (B3LYP/6-311++g(d,p)) and experimental overall geometry of ClCCCN.

B3LYP level in conjunction with 6-311++g(d,p) basis set is calculated to be 5.3625 Å which differs from the average experimental value by a factor of 0.0002 Å. Thus, it is to say that the over-all r_s -structure is a good approximation to the over-all bond length at the correlated level B3LYP/6-311++g(d,p) within, say, 0.001 Å, which is mostly under the statistical uncertainties.

Interestingly, our B3LYP/6-311++g(d,p) level optimized geometry leads to satisfactory values of rotational constants of ClCCCN shown in Table 3. The experimental values are also given for compari-

TABLE III: Comparison of the rotational constants of all the isotopomers of ClCCCN calculated at B3LYP/6-311++g(d,p) level against their experimental values²³.

Isotopic Species	Calc.	Scaled ^a	Expt.
³⁵ ClCCCN	1382.602	1382.339	1382.328(2)
³⁵ Cl ¹³ CCCN	1381.751	1381.488	1381.454(2)
³⁵ ClC ¹³ CCN	1380.607	1380.346	1380.357(2)
³⁵ ClCC ¹³ CN	1366.338	1366.090	1366.054(2)
³⁵ ClCCC ¹⁵ N	1344.232	1344.005	1343.913(2)
³⁵ Cl ¹³ CCC ¹⁵ N	1343.295	1343.068	
³⁵ ClC ¹³ CC ¹⁵ N	1342.535	1342.309	
³⁵ ClCC ¹³ C ¹⁵ N	1329.395	1329.181	
³⁵ Cl ¹³ C ¹³ CCN	1379.727	1379.466	
³⁵ Cl ¹³ C ¹³ CC ¹⁵ N	1341.571	1341.346	
³⁵ Cl ¹³ CC ¹³ CN	1365.420	1365.173	
³⁵ Cl ¹³ CC ¹³ C ¹⁵ N	1328.391	1328.178	
³⁵ ClC ¹³ C ¹³ CN	1364.517	1364.271	
³⁵ ClC ¹³ C ¹³ C ¹⁵ N	1327.846	1327.634	
³⁵ Cl ¹³ C ¹³ C ¹³ CN	1363.571	1363.325	
³⁵ Cl ¹³ C ¹³ C ¹³ C ¹⁵ N	1326.817	1326.790	
³⁷ ClCCCN	1350.544	1350.311	1350.360(2)
³⁷ Cl ¹³ CCCN	1349.888	1349.655	1349.692(2)
³⁷ ClC ¹³ CCN	1348.379	1348.148	1348.202(2)
³⁷ ClCC ¹³ CN	1334.300	1334.082	1334.089(2)
³⁷ ClCCC ¹⁵ N	1312.831	1312.633	1312.603(2)
³⁷ Cl ¹³ CCC ¹⁵ N	1312.099	1311.901	
³⁷ ClC ¹³ CC ¹⁵ N	1310.977	1310.780	
³⁷ ClCC ¹³ C ¹⁵ N	1298.001	1297.827	
³⁷ Cl ¹³ C ¹³ CCN	1347.697	1347.466	
³⁷ Cl ¹³ C ¹³ CC ¹⁵ N	1310.220	1310.024	
³⁷ Cl ¹³ CC ¹³ CN	1333.585	1333.367	
³⁷ Cl ¹³ CC ¹³ C ¹⁵ N	1297.209	1297.025	
³⁷ ClC ¹³ C ¹³ CN	1332.317	1332.108	
³⁷ ClC ¹³ C ¹³ C ¹⁵ N	1296.302	1296.119	
³⁷ Cl ¹³ C ¹³ C ¹³ CN	1331.576	1331.360	
³⁷ Cl ¹³ C ¹³ C ¹³ C ¹⁵ N	1295.486	1295.304	

^a Scaled using the slopes and intercepts obtained from the linear regression analysis.

%) than the experimental B_o values of all the 10 different isotopomers, whereas these values calculated in conjunction with other basis sets are far off (summarized in Table 1). Thus, the agreement between the theoretical prediction and experimental observation of rotational constants clearly indicates that the B3LYP/6-311++g(d,p) optimized average geometry, shown in Fig 1, is realistic and advocates for a decent predictive power of the computational procedure applied to Cl-

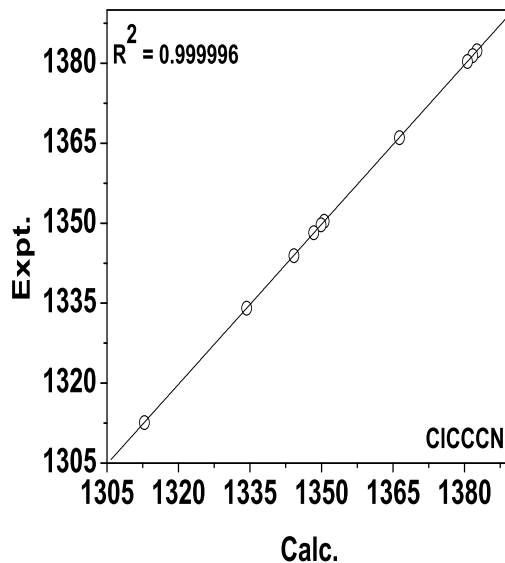


FIG. 2: Comparison between the calculated (B3LYP/6-311++g(d,p)) and experimental rotational constants of ClCCCN. The slopes and intercepts obtained from the linear regression analysis are 0.99907 and 1.02283 respectively.

analysis, shown in Figures 2, between the calculated and experimental B_o values, rotational constants of other 22 rare isotopomers of ClCCCN has been predicted accurately having standard deviation ± 0.048 MHz. A closer look at the Table 1 indicates that the HF-SCF wave functions predict dipole moments of ClCCCN close to its experimental value, deviation being 0.4 D where as the DFT wave functions overestimates it by a factor of 0.72 D irrespective of the basis sets used. Zero point vibrational effects are not taken into consideration in all these calculations.

The nuclear quadrupole coupling constants (NQCCs) of ³⁵Cl, ³⁷Cl and ¹⁴N of ClCCCN, NQCC being proportional to the electric field gradient (EFG), are calculated by using equation (8). Calculation of EFGs being made on the r_s -structures²³ as well as on the B3LYP and B3PW91/6-311++g(d,p) optimized geometries of ClCCCN. The methods, basis sets and procedures⁷ used during the calculation were B3PW91/6-311+g(df,pd) for nitrogen and B1LYP/TZV(3df,2p) for chlorine respectively. The coefficients $(eQ/h)_{eff}$ in equation (8), obtained from the linear regression analysis between the calculated EFGs and experimental NQCCs for a series of molecules containing chlorine and nitrogen, are reported⁷ to be 4.5586(40) MHz/a.u., -19.185 MHz/a.u. and -15.120 MHz/a.u. for ¹⁴N, ³⁵Cl and ³⁷Cl respectively. The nuclear quadrupole coupling constants of ³⁵Cl, ³⁷Cl and ¹⁴N are calculated on the r_s structure is

geometries are also included in Table 2 for comparison. As can be seen, the values of NQCCs deviates from the experimental values by a factor of 4.57 MHz (6.09 %) and 0.94 MHz (1.5 %) for ^{35}Cl and ^{37}Cl respectively. These deviations are significantly due to the largest error ± 4 MHz and ± 3 MHz present in the measurement of the quadrupole hyperfine structures of ^{35}Cl and ^{37}Cl of ClCCCN, though the calculated values are within the scale length of experimental uncertainties. A comparison of NQCCs of Chlorine calculated on the B3PW91/6-311++g(d,p) geometry as well as on the r_s structure reveals an almost similar value, which is basically due to the similar C-Cl bond length, whereas its value calculated on the B3LYP/6-311++g(d,p) optimized geometry is a bit off as expected since NQCC varies linearly with C-Cl bond length. A comparison with ClCN¹⁴ shows an underestimation in the value of NQCC of Cl, which being supported by a decrease of C-Cl bond length, the decrease being within 5%. On the other hand, the nuclear quadrupole coupling constant of ^{14}N of ClCCCN is also summarized in Table 2. As can be seen, the values of NQCCs of ^{14}N are very similar to each other since the r_s structure as well as the optimized B3LYP, B3PW91/6-311++g(d,p) C \equiv N structures are predicted to be very similar. Finally, comparing FCCCN⁷, HCCCN and DCCCN⁴⁰ with that of ClCCCN reveals a similar C \equiv N structure resulting a similar value of NQCC. Thus, the accurate values of NQCCs of ^{35}Cl , ^{37}Cl and ^{14}N are those derived from the r_s structures. Variations of NQCCs of ^{35}Cl and N of ClCCCN calculated directly by various levels are also summarized in Table 1.

ClCCCN has, in principle, ten fundamental modes. These modes under the C_v point group symmetry are distributed among four stretching vibrations of Σ^+ species and six bending vibrations of Π species, out of which three Π species are doubly degenerate. Thus, the vibrational assignments of ClCCCN reported by the co-authors^{24,25,26} comprises seven fundamental modes ν_1 , ν_2 , ν_3 , ν_4 , ν_5 , ν_6 and ν_7 which is in consistent with the HF and DFT level calculations. All the normal modes are calculated to be Raman active. Harmonic frequencies have been calculated at the RHF and DFT levels in conjunction with three different basis sets with increasing size in solution (benzene) as well as in vapour phase are summarized in Table 5. Experimental values are also included for comparison. All the predicted vibrational spectra have no imaginary frequency, implying that the optimized geometry is locating at the global minimum of the potential energy hyper-surface for both the methods. Frequencies calculated at the Hartree-Fock level contain known systematic errors due to the lack of electron correlation and the choice of the basis sets used, resulting an overestimation of 10-12 %. Therefore, it is usual to scale stretching frequencies predicted at

values to a high degree accuracy for a wide range of systems⁴¹. However, the improvement of the quality of the unscaled normal mode frequencies is significant in going from the non-correlated to the correlated level of theory and enlarging the size of the basis sets at the cost of its computational expanse. A comparison of the experimental values against the resulting IR normal mode frequencies calculated at the B3LYP level leads to a largest over-all error with 6-311++g(d,p) basis set is 32 cm^{-1} , with the aug-cc-pVDZ basis set the over-all error is 16 cm^{-1} whereas with aug-cc-pVTZ the over-all error is 18 cm^{-1} . An unexpected change of the ν_6 fundamental frequency has been noticed both at the B3LYP and B3PW91 levels of calculation when 6-311++g(d,p) results being compared against the aug-cc-pVNZ (N = D, T) results indicating that this mode is sensitive to the size of the basis sets used. Thus, the size of the aug-cc-pVDZ basis set is somewhat more precise for the prediction of normal mode frequencies of ClCCCN at the DFT levels of theory. The values of ν_1 , ν_2 , ν_3 , ν_4 and ν_5 computed at B3LYP/aug-cc-pVDZ are overestimated from their respective experimental values by 85.1 cm^{-1} , 49.8 cm^{-1} , 25.1 cm^{-1} , 13.7 cm^{-1} , 13.2 cm^{-1} , whereas ν_6 and ν_7 are underestimated by a factor of 21.4 cm^{-1} and 7.4 cm^{-1} . These discrepancies can be corrected either by computing an-harmonic force constants or introducing a scaled field or directly scaling the calculated wave-numbers by taking the ratio between the calculated and observed frequencies for a particular type of motion. B3LYP scaling factor for stretching modes are all close to 0.965 published elsewhere⁴². Similarly, the normal mode frequencies calculated at the DFT-B3PW91 level of theory slightly overestimated from the DFT-B3LYP values, differences, for example, being 2.9, 2, 1.3, 8.8, 15.6, 9.3 and 13.6 cm^{-1} for ν_7 ...and ν_1 respectively in conjunction with aug-cc-pVDZ basis set, whereas this overestimation is highly overestimated for stretching and bending modes computed at the HF level of theory, differences being 20.9, 86.2, 84.7, 23.6, 36.2, 235.1 and 269.7 cm^{-1} respectively. A comparison of the normal mode frequencies calculated at the B3LYP/aug-cc-pVDZ in solution (benzene) with those of gas phase values indicates a shift of C \equiv N stretching frequency towards the high wavelength region as expected whereas for other modes the shift is rather small which being in good agreement with the experimental shifts. On the other hand, a frequency calculation at the MP₂ level in conjunction with a medium size basis set 6-311++g(d,p), presented in Table 5, predicts two negative frequencies (saddle point of order two) corresponding to the -C \equiv C-Cl doubly degenerate bending mode (ν_7) and thus it was difficult to calculate the harmonic frequencies of these modes at this level.

The infrared band intensities I_i , on the other hand, of ClCCCN corresponding to the seven vibrational modes

TABLE IV: RHF, B3LYP and B3PW91 level (in conjunction with 6-311++g(d,p) (A), aug-cc-PVDZ (B), aug-cc-PVTZ (C)) calculated atomic mean dipole derivatives (\bar{p}_α), tensor anisotropies (β_α), charge undeformability ($\bar{p}_\alpha/\beta_\alpha$) and effective charges (χ_α), Mullikan Charges (${}^M q_\alpha$) of $C l_1 C_2 C_3 C_4 N_5$ in the unit of e.

Invariants	RHF			B3LYP			B3PW91		
	A	B	C	A	B	C	A	B	C
\bar{p}_{Cl}	-0.144	-0.128	-0.126	-0.158	-0.148	-0.145	-0.165	-0.154	-0.150
\bar{p}_C	0.398	0.383	0.385	0.398	0.394	0.395	0.410	0.4021	0.403
\bar{p}_C	-0.259	-0.266	-0.276	-0.228	-0.243	-0.252	-0.231	-0.247	-0.257
\bar{p}_C	0.395	0.408	0.418	0.341	0.345	0.359	0.333	0.342	0.354
\bar{p}_N	-0.390	-0.397	-0.401	-0.353	-0.348	-0.357	-0.347	-0.340	-0.350
β_{Cl}	0.753	0.725	0.725	0.926	0.873	0.864	0.956	0.896	0.886
β_C	1.246	1.229	1.231	1.430	1.338	1.329	1.465	1.361	1.352
β_C	0.835	0.813	0.816	0.890	0.817	0.809	0.903	0.819	0.814
β_C	0.556	0.487	0.478	0.558	0.490	0.475	0.562	0.483	0.467
β_N	0.214	0.179	0.168	0.173	0.139	0.131	0.168	0.129	0.119
\bar{p}_{Cl}/β	-0.191	-0.176	-0.174	-0.171	-0.169	-0.168	-0.173	-0.172	-0.169
\bar{p}_C/β	0.319	0.312	0.313	0.278	0.294	0.297	0.280	0.295	0.298
\bar{p}_C/β	-0.310	-0.327	-0.338	-0.256	-0.297	-0.311	-0.256	-0.302	-0.316
\bar{p}_C/β	0.710	0.838	0.874	0.611	0.704	0.756	0.592	0.708	0.758
\bar{p}_N/β	-1.822	-2.218	-2.387	-2.040	-2.504	-2.725	-2.005	-2.636	-2.941
$ \chi_{Cl} $	0.383	0.365	0.364	0.464	0.437	0.432	0.480	0.449	0.444
$ \chi_C $	0.710	0.694	0.697	0.783	0.744	0.741	0.804	0.757	0.754
$ \chi_C $	0.471	0.467	0.473	0.477	0.455	0.457	0.483	0.458	0.462
$ \chi_C $	0.474	0.469	0.474	0.430	0.416	0.423	0.425	0.410	0.417
$ \chi_N $	0.403	0.406	0.409	0.362	0.354	0.362	0.355	0.348	0.354
${}^M q_{Cl}$	0.387	-0.208	-0.063	0.463	-0.030	0.042	0.510	-0.137	-0.003
${}^M q_C$	0.082	-0.898	-0.901	0.035	-0.661	-0.877	0.101	-0.678	-0.820
${}^M q_C$	1.954	1.838	1.985	1.648	1.155	1.656	1.749	1.367	1.529
${}^M q_C$	-2.139	-0.387	-0.632	-1.969	-0.214	-0.447	-2.154	-0.214	-0.252
${}^M q_N$	-0.283	-0.344	-0.389	-0.177	-0.249	-0.374	-0.207	-0.338	-0.454

very strong, strong, very weak, weak, strong, medium strong, and very weak respectively. The calculated intensities are summarized in Table 7. As can be seen, the most intense absorption infrared band (I_1) corresponds to the $C\equiv N$ normal mode as expected irrespective of the methods and basis sets used, variation in intensity is within 30 km/mole between the two (HF-SCF and DFT) theoretical methods. For the band I_2 , the differences between the RHF and B3LYP values in intensity are within 20 km/mole. Out of the three doubly degenerate bending modes, intensities of I_6 and I_5 corresponding to the normal modes ν_5 and ν_6 are calculated to be of equal in magnitude which were experimentally assigned to be medium strong and strong respectively. As shown in Table 6, the main discrepancy in intensity is found for the $\equiv C-C\equiv$ stretching band I_3 . For this band, variations in intensities are within 6-13 km/mole between the two theoretical methods. A comparison of IR intensities calculated (for example, at the B3LYP/aug-cc-pVDZ

indicates a significant enhancement of $C\equiv N$ stretching intensity as expected, since intensities measured in solutions somewhat larger than the gas phase intensities¹⁰, whereas for other bands the change is very less. Thus, the agreement between the calculated and the experimental gauss treatment in intensities, is far from being quantitative. Since there is no quantitative experimental data on IR intensity measurements for all these bands, no satisfactory interpretation could have possible. However, a direct calculation of the dipole moment derivative with respect to the normal co-ordinates can serve the purpose. For, one makes the use of APT analysis that permits the interpretation of IR intensities by means of mean atomic charges (\bar{p}_α), the mass-weighted square effective charges ($\frac{\chi_\alpha^2}{m_\alpha}$), where m_α and χ_α are the mass and effective charge of each atom α of ClCCCN, since all these invariants are related to each other by the well known relation called as the G-sum rule⁴³ given by: $\sum_{\alpha} I_{\alpha} = 0.719 \sum_{\alpha} \frac{3\chi_{\alpha}^2}{m_{\alpha}}$ where α is the rotational

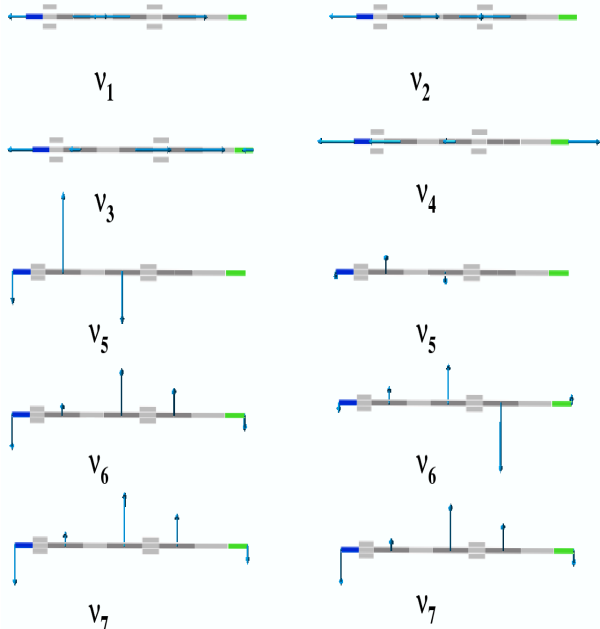


FIG. 3: Normal modes (summarized in Table 5) of ClCCCN. Atomic numbering is shown in Figure 1. The modes corresponding to $\nu_5 - \nu_7$ are repeated twice since these are doubly degenerate. The actual directions of vibrations of the doubly degenerate bending modes were out of (shown as up) and into (shown as down) the paper which being modified here for a clear visualization of these modes.

it permit a direct calculation of atomic polar charges.

The mean atomic charges as well as the other rotational invariants derived from the atomic polar tensors (APTs) using equations (1) to (5) for all the five atoms of the ClCCCN are summarized in Table 4. The atomic polar charges \bar{p}_α represent the redistribution of the electric charge density around each atom in such a way that their sum over all atoms equal to zero in the molecular bonding environment of ClCCCN at its optimized equilibrium geometry. An important difference between APT charges and the Mulliken charges^{44,45} is that the basis-set dependence of the former arises only from the fact that the basis set can be incomplete; hence, as the basis set approaches completeness, the APT charges approach a well-defined limit⁴⁶. A test with ClCCCN, shown in Table 4, clearly indicates that GAPTs are almost invariant with respect to the basis sets. The polar tensor elements are calculated to be all negative for chlorine and nitrogen atoms as expected since these are the electronegative elements, contrast to the carbon atom (C_4) attached to it through a triple bond character which is highly positive, resulting the mean dipole moment of nitrogen as negative and that of carbon as positive, each of which can be interpreted as carrying slightly more than $-0.35 e$ and $+0.35 e$. This, in turn, results in an unequal distribution of charges

almost equal amount of positive charge on the other carbon atom C_2 , leading to an interpretation that the carbon atoms C_3 and C_2 carries atomic charges slightly more than $+0.25e$ and $-0.25e$ respectively. The average values of atomic polar charges calculated by all the methods are $-0.146e$, $0.396e$, $-0.251e$, $0.366e$ and $-0.365e$ having standard deviations $\pm 0.013e$, $\pm 0.001e$, $\pm 0.0016e$, $\pm 0.032e$ and $\pm 0.024e$ for Cl, C, C, C, N of ClCCCN respectively which indicates an overestimation of standard deviations of C_4 and N that arises mainly due to p_{zz} component of the atomic polar tensors of C and N. It is noted worthy that all other invariant quantities are within $0.1e$ whereas a larger variation in the value of anisotropy parameter β as well as in the value of undeformability of charge (\bar{P}/β) on the atom α of ClCCCN (as shown in Table 4) has been noticed.

The Mulliken atomic charges, on the other hand, of chlorine and carbon attached each other by means of a single bond are predicted to be positive in conjunction with 6-311++g(d,p) basis set at all the methods, whereas these are predicted to be negative in conjunction with aug-cc-pVNZ (N = D, T) basis sets. Similarly, the charge of carbon atom attached to the nitrogen atom through a triple bond character is predicted to be negative irrespective of the methods and basis sets used. However, it successfully predicted a real sign to the nitrogen atom as expected. As can be seen, variations of these charges with respect to all the methods as a function of basis set choice is rather large, variations being $-0.208e$ to $0.51e$, $-0.898e$ to $0.101e$, $1.155e$ to $1.985e$, $-0.387e$ to $-2.154e$ and $-0.117e$ to $0.454e$ for Cl, C, C, C and N of ClCCCN respectively, whereas APT charges are less variable irrespective of the methods and basis sets used. A comparison of APT charges with the Mulliken atomic charges indicates that the APT charges are highly reliable than the Mulliken atomic charges and the Mulliken population analysis of atomic charge densities of ClCCCN does not reflect the physical and chemical characteristics of this system under consideration. Finally, a comparison of the Mulliken atomic charges with the effective charges (χ), shown in Table 4, reveals an increase of Chlorine(Cl), C_2 , C_4 and N_5 APT charges as M_q diminishes, which leads to an interpretation that χ is dominated by the stretching intensities⁴⁷.

IV. CONCLUSION

All the spectroscopic constants were calculated at the restricted HF-SCF as well as DFT (B3LYP, B3PW91) levels in conjunction with a variety of basis sets. Satisfactory agreements between the B3LYP/6-311++g(d,p) and experimental values of rotational constants were found for ClCCCN. Over-all, $r_{Cl...N}$, bond distance is a good approximation to the over-all bond distance at the corre-

TABLE V: Comparison of the normal mode frequencies^a (in cm^{-1}) of ClCCCN calculated at all the three different levels of theory with their corresponding experimental values. Here A, B, and C stands for 6-311++g(d,p), aug-cc-pVDZ and aug-cc-pVTZ basis sets respectively.

ν_i	Species	Motion ^b	RHF			B3LYP			B3PW91			MP ₂	Expt. ^c	Expt. ^d
			A	B	C	A	B	C	A	B	C	A		
1	Σ^+	$-C \equiv N$ st.	2652.9	265.9	2644.3	2384.4	2382.2	2375.9	2397.3	2395.8	2386.7	2263.7	2297	2283
2	Σ^+	$-C \equiv C$ st.	2477.0	2478.9	2474.6	2248.3	2243.8	2249.2	2256.8	2253.1	2256.0	2087.6	2194	2195
3	Σ^+	$\equiv C-C \equiv$ st.	1152.6	1154.4	1148.4	1116.5	1118.2	1115.1	1132.6	1133.8	1129.5	1112.6	1093	1099
4	Σ^+	$\equiv C-Cl$ st.	563.4	564.4	563.0	540.1	540.8	541.3	549.1	549.6	549.3	538.2	527	528
5	Π	$\equiv C-C \equiv N$ bd.	582.8	580.9	615.6	507.3	496.2	535.2	511.9	497.5	536.8	412.6	483	482
6	Π	$\equiv C-C \equiv C-$ bd.	379.1	397.8	423.5	268.2	311.6	361.6	268.0	313.6	364.8	129.9	333	332
7	Π	$-C \equiv C-Cl$ bd.	150.0	142.4	150.5	135.7	121.5	137.0	135.4	123.4	137.5	<u>434.2</u>	129	140

^a Unscaled harmonic frequencies.

^b st. = stretching; bd. = bending.

^c Ref.^{25,26}. Normal mode frequencies observed in vapour phase.

^d Ref.^{25,26}. Normal mode frequencies were observed in benzene. For comparison, the values of the normal modes are calculated at the B3LYP/aug-cc-pVDZ level of theory in solution (benzene) to be 2374.2, 2239.4, 1121.6, 542.10, 500.7, 313.1 and 121.9 cm^{-1} for ν_1 and ν_7 respectively.

TABLE VI: Comparison of the IR intensities (in Km/mol) of ClCCCN calculated at the HF and DFT levels with corresponding experimental values. Here A, B, and C stands for 6-311++g(d,p), aug-cc-pVDZ and aug-cc-pVTZ basis sets respectively.

I_i	RHF			B3LYP			B3PW91			MP ₂	$A_{expt.}^a$	$A_{expt.}^b$
	A	B	C	A	B	C	A	B	C	A		
1	195.05	190.18	185.27	215.44	200.78	194.59	219.57	201.19	195.93	155.84	vs	vs
2	38.88	33.34	40.98	27.41	19.47	26.30	31.02	21.94	28.92	18.84	w	w
3	16.26	15.10	14.47	25.40	22.60	21.74	27.12	23.74	22.60	16.14	s	s
4	5.49	4.73	4.77	8.15	7.15	7.01	8.23	7.17	7.01	8.11	m	m
5	9.20	10.70	9.62	5.98	7.91	6.93	5.44	7.94	6.84	8.68	s	s
6	4.54	7.37	10.16	5.22	4.26	7.37	4.88	4.03	7.08	2.36	m	m
7	4.87	5.01	4.91	3.90	3.78	3.54	3.86	3.61	3.38	1.26	vw	vw
Sum	274.29	266.43	270.18	299.0	265.95	267.48	291.50	269.48	271.76	211.23		

^a Ref.^{25,26}. vs = very strong, s = strong, m = medium strong; vw = very weak; w = weak.

^b Ref.^{25,26}. For comparison, the IR intensities are calculated at the B3LYP/aug-cc-pVDZ level of theory in solution (benzene) to be 428.7, 21.8, 33.6, 10.2, 12.6, 4.2 and 5.4 cm^{-1} for A_1 ... and A_7 respectively.

the B1LYP/TZV(3df,3p) and B3LYP/6-311++g(df,pd) levels respectively on the r_s structure as well as on the B3PW91/6-311++g(d,p) optimized geometry are well within the scale length of experimental uncertainty. Enlarging basis sets size could improve the calculation accuracy and satisfactorily reproduced the experimental bending mode frequencies without being scaled with uniform scaling factors, though the stretching frequencies are a bit off. The rotational invariants have been satisfactorily explained at these levels of theory. The sta-

theory is not a true minimum rather a saddle point of order two and thus scan of the potential energy surface should be emphasized in order to determine the nature of the saddle point and verify any possible existence of conical intersection between the ground and first excited state.

Acknowledgments. The author would like to thank Dr. Nikhil Guchhit of University of Calcutta, for kindly allowing to use Gaussian 03 suite program package and Dr. P. R. Bangal for helpful discussions in connection with Gaussian.

- * Electronic address: pr.varadwaj@saha.ac.in
- ¹ S. Thorwirth, M. C. McCarthy, J. B. Dudek, P. Thaddeus, *J. Chem. Phys.* 122 (2005) 184308.
 - ² S. G. Kukolich, C. Tanjaroorn, *J. Chem. Phys.* 119 (2003) 4353.
 - ³ A.C. Cheung, D.M. Rank, C.H. Tonwes, W.J. Welch, *Nature* 221 (1969) 917.
 - ⁴ M.J. Travers, W. Chen, S.E. Novick, J.M. Vrtilik, C.A. Gottlieb, P. Thaddeus, *J. Mol. Spectrosc.* 180 (1996) 75.
 - ⁵ D.J. DeFrees, A.D. McLean, *J. Chem. Phys.* 82 (1985) 333.
 - ⁶ Y. Yamaguchi, H.F. Schaefer III, *J. Chem. Phys.* 73 (1980) 2310.
 - ⁷ <http://turbo.kean.edu/~wbailey/NQCC.html>; References there in.
 - ⁸ H. L. Skriver, *Phys. Rev. B* 31 (1985) 1909.
 - ⁹ R. Kolos, A. L. Sobolewski, *Chem. Phys. Lett.* 344 (2001) 625.
 - ¹⁰ S. R. Polo, M. K. Wilson, *J. Chem. Phys.* 23 (1955) 2376.
 - ¹¹ R. L. A. Haiduke, A. E. Oliveira, R. E. Bruns, *J. Phys. Chem. A* 104 (2000) 5320; References there in.
 - ¹² Pradeep R. varadwaj, Prakriti R. Bangal, *J. Mol. Struct.:Theochem* (in press).
 - ¹³ S. Blanco, J. C. Lopez, M. E. Sanz, A. Lesarri, H. Dreisler, J. L. Alonso, *J. Mol. Spectrosc.* 227 (2004) 202.
 - ¹⁴ Pradeep R. Varadwaj, Prakriti R. Bangal, A. I. Jaman, *J. Mol. Struct.* (in press).
 - ¹⁵ Pradeep R. varadwaj, A. I. Jaman, L. Pszczolkowski, Z. Kisiel, (Manuscript in preparation).
 - ¹⁶ P. Thaddeus, M. C. McCarthy, *Spectrochim Acta A* 57 (2001) 757.
 - ¹⁷ Cologne Database for molecular spectroscopy, <http://www.phl.uni-koeln.de/vorhersagen>.
 - ¹⁸ M. B. Bell, M. J. Travers, M. C. McCarthy, C. Gottlieb, P. Thaddeus, P. A. Feldman, *APJ.* 483 (1997) L61.
 - ¹⁹ T. Okabayashi, M. Tanimoto, K. Tanaka, *J. Mol. Spectrosc.* 174 (1995) 595; References there in.
 - ²⁰ Pradeep R. Varadwaj, A. I. Jaman, *J. Mol. Spectrosc.* 227 (2004) 23-27.
 - ²¹ Pradeep R. Varadwaj, A. I. Jaman, International Conference on Submillimeter Science and Technology (ICSST-04), PRL, India, (2004) abs. 22.
 - ²² A. I. Jaman, *Pramana: J. Phys.* 6(1) (2003) 85.
 - ²³ T. Bjorvatten, *J. Mol. Struct.* 20 (1974) 75.
 - ²⁴ S. J. Cyvin, E. Kloster-Jensen, P. Klaboe, *Acta Chem. Scand.* 19 (1965) 903.
 - ²⁵ D.H. Christensen, I. Johnsen, P. Klaboe, E. Kloster-Jensen, *Spectrochim. Acta* 25A (1969) 1569.
 - ²⁶ P. Klaboe, E. Kloster-Jensen, *Spectrochim. Acta* 23A (1967) 1981.
 - ²⁷ W.T. King, G.B. Mast, P.P. Blanchette, *J. Chem. Phys.* 56 (1972) 4440; *ibid.*, 58 (1973) 1272.
 - ²⁸ W.T. King, G.B. Mast, *J. Chem. Phys.* 80 (1976) 2521.
 - ²⁹ W.B. Person, *Vibrational Intensities in Infrared and Raman Spectroscopy*, chapter 4 and 14; W.B. Person and G. Gerbi (1982) Eds., Elsevier, Amsterdam.
 - (b) W.B. Person, J.H. Newton, *J. Chem. Phys.* 61 (1974) 1040.
 - ³⁰ A.D. Becke, *J. Chem. Phys.* 98 (1993) 5648.
 - ³¹ J.P. Perdew, K. Burke, Y. Wong, *Phys. Rev. B* 54 (1996) 16533.
 - ³² A.D. Becke, *J. Chem. Phys.* 104 (1996) 1040.
 - ³³ C. Adamo, V. Barone, *Chem. Phys. Lett.* 274 (1977) 242.
 - ³⁴ T. J. Dunning, *J. Chem. Phys.* 90 (1989) 1007; R. A. Kendall, T. H. Dunning, R. J. Harrison, *ibid.* 96 (1992) 6796.
 - ³⁵ A. Schafer, C. Huber, R. Ahlrichs, *J. Chem. Phys.* 100 (1994) 5829.
 - ³⁶ Gaussian 03, Revision B.03, Gaussian, Inc., Pittsburgh PA, (2003).
 - ³⁷ E.B Wilson, J.C. Decius and P.C. Cross, *Molecular Vibrations*, McGraw-Hill, New-York (1955).
 - ³⁸ J. Overend; In *Infrared Spectroscopy and Molecular Structure*; Davis, M.,Ed., Elsevier; New-York: Chapter 10 (1963).
 - ³⁹ P. Carsky, V. Spirko, B. Andes Hess Jr., L. J. Schaad, *J. Phys. Chem.* 94 (1990) 5493.
 - ⁴⁰ E. Fleiege, H. Dreizler, B. Kleibomer, *J. Mol. Struct.* 97 (1983) 225.
 - ⁴¹ J.B. Foresman and A. Frisch, *Exploring Chemistry with Electronic Structure Methods*, Gaussian, Inc. Pittsburgh, USA (1996).
 - ⁴² A.P. Scott, *L. Radom J. Chem. Phys.* 100 (1996) 16502.
 - ⁴³ B. Crawford Jr., *J. Chem. Phys.* 20 (1952) 977.
 - ⁴⁴ R.S. Mulliken, *J. Chem. Phys.* 23 (1955) 1833, 1841, 2338, 2343; (1962) 32, 326.
 - ⁴⁵ P. Politzer, R.S. Mulliken, *J. Chem. Phys.* 55 (1971) 5135.
 - ⁴⁶ J. Cioslowski, P.J. Hay, J.P. Ritchie, *J. Phys. Chem.* 94 (1990) 148.
 - ⁴⁷ D. C. McKean, A. Kindness, N. Wilkie and W. F. Murphy, *Spectrochim Acta* 52 (1996) 445.